HOKKAIDO UNIVERSITY

Title	Metastable Structure of Photoexcited WO3 Determined by the Pump-probe Extended X-ray Absorption Fine Structure Spectroscopy and Constrained Thorough Search Analysis
Author(s)	Kido, Daiki; Uemura, Yohei; Wakisaka, Yuki et al.
Citation	Chemistry Letters, 51(11), 1083-1086 https://doi.org/10.1246/cl.220381
Issue Date	2022-11
Doc URL	https://hdl.handle.net/2115/90216
Type	journal article
File Information	WO3_manuscript_2nd_kido.pdf

Hokkaido University Collection of Scholarly and Academic Papers : HUSCAP

Metastable structure of photoexcited WO_3 determined by the pump-probe extended X-ray absorption fine structure spectroscopy and constrained thorough search analysis

Daiki Kido,[1] Yohei Uemura,[2] Yuki Wakisaka,[2] Akihiro Koide,[2] Hiromitsu Uehara,[1] Yasuhiro Niwa,[3] Shunsuke Nozawa,[3] Kohei Ichiyanagi,[3] Ryo Fukaya,[3] Shin-ichi Adachi,[3] Tokushi Sato,[4] Harry Jenkins,[5] Toshihiko Yokoyama,[2] Satoru Takakusagi,[1] Jun-ya Hasegawa,[1] and Kiyotaka Asakura*[1]

[1]*Institute for Catalysis Hokkaido University, Kita21, Nishi10, Kita-ku, Sapporo, 001-0021, Hokkaido, Japan*
[2]*Institue for Molecular Scinence, 38 Nishigo-Naka,Myodaiji, Okazaki, 444-8585, Aichi, Japan*
[3]*Photon Factory, Institute for Materials Structure Science, 1-1 Oho,, Tsukuba, 305-0801, Ibaraki, Japan*
[4]*European XFEL GmbH, 4, Holzkoppel, 22869, Schenefeld, Germany*
[5]*Cardiff Catalysis Institute, Cardiff University, , Cardiff, CF10 3AT, Wales, UK*

E-mail: askr@cat.hokudai.ac.jp

The local structure of WO_3 photocatalyst in the photoexcited metastable state created 150 ps after laser irradiation have been determined by the pump-probe L_3-edge EXAFS and the constrained thorough search analysis. A highly distorted octahedral local structure was found where one of the shortest W-O bonds was further shortened to 1.66 Å while the other five bonds were rather elongated even though theoretical calculations predicted the reverse change. We discuss this contradiction and propose a possible structure for the metastable state.

Keywords: Photocatalyst, Pump-probe EXAFS, Thorough search method

Photocatalysts are paid attention to harvest sunlight to split water into H_2 and O_2.[1] Many kinds of researches have been carried out to improve the efficiency of photocatalyst such as impurity doping, Z-scheme method, and so on. Usually, these processes are understood in the energy band model. In the energy band model, the positions of Fermi level, minimum of the conduction band, and maximum of valence band are important against the reduction and oxidation potentials for H_2/H_2O and O_2/H_2O. The local structure and electronic state of the photoexcited state need to be elucidated to understand the photocatalysis of water splitting and to improve the performance of water-splitting photocatalysts.

A pump–probe (PP) X-ray absorption fine structure (XAFS) investigation of the photocatalysts using pulsed X-rays emitted from an X-ray free electron laser (XFEL) and synchrotron radiation (SR) has revealed element-specific local electronic and geometrical structures, thereby providing new scientific knowledge about photocatalysis that cannot be obtained by other techniques.[2] WO_3 is used as a Z-scheme water-splitting photocatalyst that is sensitive to visible light, which is the main component of sunlight.[3] We have acquired PP X-ray absorption near edge structure (PP-XANES) spectra of WO_3 after pulsed laser irradiation and have found that the valence change of W ion just after laser irradiation (<500 fs) then the metastable state (MS) was created within 150 ps followed by relaxation to the ground state (GS) with a time constant of 2 ns.[4-7] We proposed that the photoelectrons were trapped at distorted stoichiometric W sites in the crystal lattice, similar to the trapping of polarons, instead of at surface or bulk defects.[6] The formation time for the MS, 150 ps, was longer than that for the other oxides such as TiO_2 and Fe_2O_3, consistent with previously-reported optical measurement results.[8] It is desirable to acquire the PP extended X-ray absorption fine structure (PP-EXAFS) spectrum to confirm the structure change because EXAFS is sensitive to local structural features such as bond lengths.[9] However, PP-EXAFS spectral measurements are much more difficult than PP-XANES measurements[6] because of the lower PP-EXAFS signal intensity. In addition, compounds with a complex structure, such as WO_3, require a multishell fitting which is inherently challenging. We addressed these two difficulties by taking the difference spectra between before and after photoabsorption to obtain the EXAFS spectrum of MS WO_3. The difference spectra were accumulated and then analyzed using the constrained thorough search (CTS) method to elucidate the bond lengths in MS WO_3.[10, 11]

In the present paper, we report the PP-EXAFS results for the structure of the MS WO_3 state to clarify the local structure change and to attempt to explain the long formation time for MS WO_3.

The WO_3 was purchased from Wako Chemicals, and 50–200 nm WO_3 particles were dispersed in ultrapure water. The concentration of WO_3 was 2.5 mmol L^{-1}. The WO_3 jet was supplied to the cross point of the laser used for photoexcitation (Ti-sapphire with a 1 ps pulse width, 945 Hz repetition rate, and 400 nm wavelength) and the X-ray beam emitted from the Photon Factory Advanced Ring (PF-AR, 6.5 GeV, 60 mA, single bunch operation with pulse width of 100 ps, and pulse interval of 1.26 μs). The fluorescence X-rays were monitored using a scintillation counter with a Cu filter to attenuate the elastic X-rays. Details of the experimental setup are available elsewhere.[4]

The difference spectrum before and after the photoirradiation, $\Delta\mu(=\mu_{API} - \mu_{BPI})$, was accumulated, thereby reducing the possible fluctuations. The μ_{API} and μ_{BPI} were the spectra recorded after and before the photoirradiation, respectively. The spectrum of the MS WO_3, μ_{MS}, was obtained by assuming that μ_{API} was a linear combination of the spectrum of the ground state (GS), μ_{GS}, and μ_{MS}. $\mu_{API} = \alpha\mu_{MS} + (1 - \alpha)\,\mu_{GS}$, where α, the fraction of MS WO_3, was obtained from the XANES spectrum, as shown in Figure S1 in the supporting information (SI-1). μ_{BPI} was equal to that of the ground state, μ_{GS}. Therefore, μ_{MS} is obtained from $\mu_{MS}= \Delta\mu/\alpha+\mu_{GS}$, which was then processed and analyzed using the EXAFS analysis programs REX2000[12] and LARCH[13], as described in SI-2. The Fourier transformation

ranges of Δk and Δr were 5 (= 8 − 3) Å^{-1} and 1 (= 2 − 1) Å, respectively, so that the amount of information, M, was approximately 5 (M = 2Δk ·Δr)/π +2).[14] The inversely Fourier transformed data were first analyzed by a curve-fitting method using the LARCH package.[13] Further details of the structure, including bond lengths, were derived from the EXAFS spectra using the CTS method, as explained in SI-4.[10,11,15]

Figure. 1 shows the EXAFS oscillation of the MS WO_3,

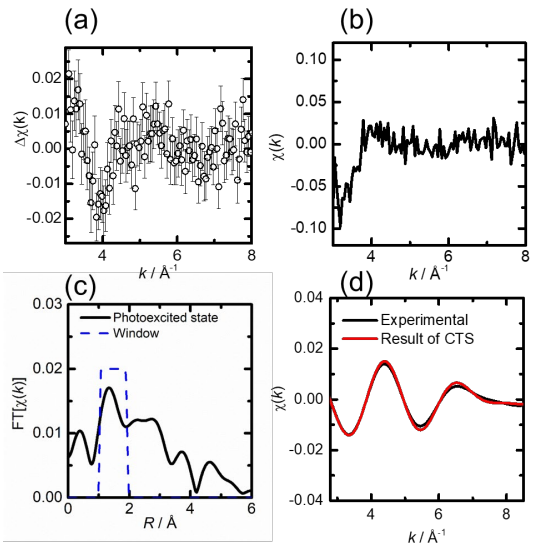

Figure 1. (a)Δχ (*k*) for W L_3-edge EXAFS spectra between before and 150 ps after the irradiation. (b) $\chi_{MS}(k)$ for the MS WO_3. (c) The Fourier transform of $\chi_{MS}(k)$. The broken line shows the range of Fourier filtering. (d) Inversely Fourier transformed data (black line) for the MS WO_3 with the results of CTS (red line). The enlarged one is available in Fig. S4

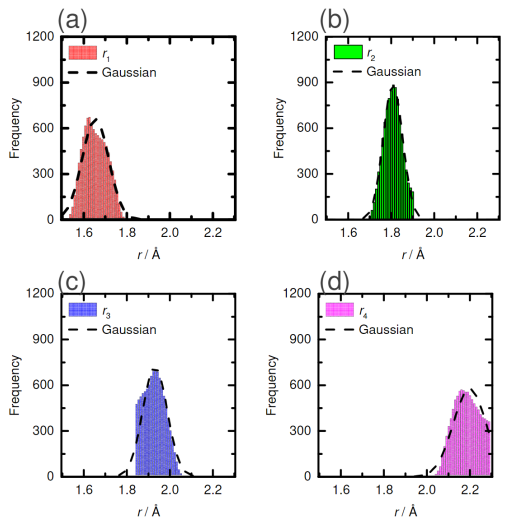

Figure 2. (a)-(d) Distribution of bond lengths that satisfy R-factor < 0.10 for the structure parameters for the MS WO_3. Dashed lines show the fitting results obtained using a Gaussian function.

$\chi(k)_{MS}$, and its Fourier transform. The main peak at 1.4 Å was inversely Fourier transformed to the k-space, and the data were analyzed by one-shell curve fitting. The one-shell curve fitting results are shown in Figure S2 and Table S1 in SI-3. We conducted the analysis using two methods. In the first method, the Debye–Waller (DW) factor was adjusted freely; in the second method, the DW factor was constrained as a function of the bond length given by Eq S5 in SI-4. Both results indicated that the bond length contracted in the MS WO_3; however, details of the structure were unclear.

We carried out the CTS analysis based on the uniform prior probability principle.[11] CTS analysis can visualize the correlations of parameters from the multi-dimensional parameter space. Especially, CTS analysis can be all candidates which reproduce the experimental data well and reject the possibility of other structures in the searched parameter space. CTS analysis was applied to extract the convincing information. We assumed the followings:

1. MS WO_3 has distorted octahedra, similar to GS WO_3.
2. DW factors are functions of the bond length in Eq S5 in SI-4.[16] A greater length corresponds to a larger DW factor.
3. EXAFS spectroscopy is sensitive to short bonds because of the $\exp(-2r/\lambda - 2\sigma^2k^2)/r^2$ term.

The structural parameters were limited to the value of M (≈5). The GS WO_3 has a monoclinic structure in which two distorted octahedral sites are present, as shown in Table S3.[17] The bond lengths in GS WO_3 have 12 different values. Two sites have a similar local structure; the corresponding W-O distances are therefore denoted as r_1''', r_2''', r_3''', r_4''', r_5''', and r_6''' in Table S3 in SI-4. We intended to demonstrate that $r_1''' \neq r_2'''$ in the MS WO_3, as predicted from the W L_1-edge XANES results.[6] According to assumption (3) (i.e., that shorter bonds (r_1''', r_2''') have greater contributions to the EXAFS spectra), we assumed that r_1''' and r_2''' were independently optimized and we constrained $r_3''' = r_4''' = r_3$ and $r_5''' = r_6''' = r_4$, as shown in Table S3. The CTS was carried out for the four parameters $r_1(=r_1''')$, $r_2(=r_2''')$, r_3, and r_4 with the corresponding coordination numbers, $N_1 = N_2 = 1$ and $N_3 = N_4 = 2$, as shown in Table S2 and Table S3 in SI-4. Table 1 shows the CTS results that reproduced the crystal data given in Table S3 in SI-4 for the GS WO_3. Note that r_1 and r_2 are approximately the same as shown in Table 1 even if the two parameters are independently changed. Figure S5 shows the occurrence histograms. We found that the histograms for r_1 and r_2 have similar distributions and the same peak positions. Consequently, for the GS WO_3, we conclude that r_1 and r_2 agreed with each other within the error.

Table 1 shows the CTS results for the MS WO_3. Figure S4 shows a comparison between the Fourier filtered $\chi(k)_{MS}$ and the calculated one. The observed data were well reproduced by the parameters determined by the CTS method. The *R*-factor (Eq S3) was 0.02. In the case of the MS WO_3, we found that r_1 and r_2 were not equal and that r_1 was 0.11 Å shorter than that for the GS WO_3.

Table 1. Results of constrained thorough search analysis for the W L_3-edge EXAFS spectra of GS and MS WO_3. "Crystal" indicates crystallographic data.[17]

Sample	r_1 / Å	r_2 / Å	r_3 / Å	r_4 / Å	*R*-factor
GS	1.77 ±0.08	1.77 ±0.08	1.91 ±0.04	2.17 ±0.09	0.049
Crystal	(1.75	1.77	1.90	2.13)	
MS	1.66 ±0.06	1.81 ±0.04	1.93 ±0.06	2.19 ±0.07	0.012

The histograms of r_1 and r_2 show different peak positions (Figure 2). The 2 dimensional frequency plot in Figure S6 clearly shows the different peak position at $r_1 \neq r_2$. Bonds other than r_1 in the MS WO_3 were longer than the corresponding bonds in the GS WO_3, in good agreement with previously reported WO_3 L_1-edge XANES results.[6] The photoexcited MS WO_3 exhibited a further distorted structure.

The CTS analysis showed that the MS WO_3 exhibited a further distorted structure, where the shortest W=O bond was further shortened from 1.77 Å to 1.66 Å. This structure change was interpreted as follows in a previous paper.[6] The photoelectron excited by the pulsed laser would occupy the d_{xy} orbital of W, which was on a plane perpendicular to the shortest W=O bond. The orbital was located at the bottom of the conduction band in energy scale, forming a π^* antibonding orbital with $2p_x$ and $2p_y$ for oxygen atoms in the xy plane. Thus, the W-O bonds in the xy plane were elongated, pushing up the W atom in the direction of the shortest W=O bond.[6] As described later and in SI-8 and in SI-9, this previous interpretation is not consistent with the results of the density functional theory (DFT) and quantum mechanics/molecular mechanics (QM/MM) calculations. This discrepancy will be discussed below.

In the literature, the MS WO_3 was assumed to be located in bulk or surface defect sites.[18-20] However, we disproved these possibilities because the amount of MS states was much larger than the amount of defects. Yamakata et al. recently reported that introducing defects by reducing WO_3 decreased the lifetime of the MS WO_3.[21] Surface defects might be less likely because the surrounding environment did not affect the lifetime of the MS WO_3, as shown in SI-7. We proposed the MS WO_3 should be located at the normal lattice sites in the bulk stoichiometric WO_3 and be distorted from the structure of the GS WO_3. Such distortion would stabilize the MS WO_3, similar to the stabilization of polarons.

However, we still faced two problems. First, the DFT and QM/MM calculations for the MS WO_3 local structure indicated that the less-distorted structure was stable, with the shortest W=O bond being elongated as shown in Table S5 in SI-8. Second, it was unclear why the formation of the MS WO_3 structure took 150 ps. The vibration frequencies of W-O are on the order of 100 cm^{-1} or 3 THz or 0.3 ps. Fe_2O_3 hematite and $CuWO_4$ took less than 1 ps to produce a polaronic MS.[22, 23] Thus, the simple isolated distorted MS structure should form much faster. According to the L_3-edge XANES result obtained from femtosecond time resolved measurement, the W^{5+} was formed and was gradually changed to the MS structure.[5] Such a long time scale might be related to the collective structure change. If the single distorted structure of the MS WO_3 was located in the GS WO_3, it should have a greater distortion energy between the surrounding GS WO_3. Thus, the theoretical calculation suggested a less distorted structure. If the two distorted MS along which the shortest W=O bonds were assumed to be headed, the distortion energy should be released. Consequently, the formation of the well-ordered distorted MS WO_3 cluster shown in Figure 3 should require a long time.

The problem with the well-ordered MS WO_3 clusters is the charge balance, which should show a large negative charge. To compensate for the negative charge, holes should combine with photoexcited electrons in the well-ordered MS WO_3 cluster. In this case, the recombination of photoexcited electrons and holes might be enhanced. If the spins of the hole and the photoexcited electron near the hole were parallel or in a triplet state, the well-ordered distorted MS cluster should be stabilized and had a finite lifetime. The large-scale DFT calculations of the MS excited state with a large cluster size or time-resolved micro X-ray Magnetic Circular Dichroism (XMCD) of O and W could support our hypothesis for the formation of such a well-defined distorted MS WO_3 cluster, which will be the future challenge.

Picosecond time-resolved W L_3-edge EXAFS spectroscopy was conducted to characterize the structural change in MS WO_3 in detail. We applied the CTS method to

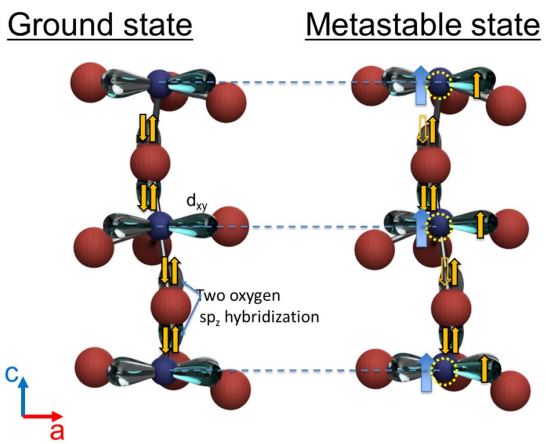

Figure 3: The local structure change in the GS WO_3 (left panel) and the MS WO_3 (right panel). Large red and small blue circles represent O and W atoms, respectively. Yellow broken circles indicate the position of W in GS. Thick blue arrows show the movement of W atoms in the MS WO_3. W atoms along the c-axis move in the direction corresponding to W=O contraction. Orange filled and empty arrows in the orbitals correspond to electrons with spin and holes, respectively. Grey filled circles indicate holes. The unpaired electron spins are all parallel in the polaron cluster.

analyze the EXAFS data for the MS WO_3, where one of the shortest bonds was further shortened by 0.11 Å from its original bond length, consistent with the structure proposed on the basis of W L_1-edge XANES spectroscopy. This structural change in the MS WO_3 led the distorted MS structure, which should be stabilized, to form well-ordered distorted clusters in conjunction with the formation of the triplet state.

The authors would like to express their gratitude to Prof. Masaaki Yoshida at Yamaguchi University for his technical advice and to the Japan Society for the Promotion of Science (JSPS) for their support through a Grant-in-Aid for Exploratory Research (No. 26620110), a Grant-in-Aid for Scientific Research (A) (Nos. 15H02173 and 20H00367), a Grant-in-Aid for JSPS Research Fellow (No. 15J07459), and a Grant for collaborative research in the Institute for Catalysis, Hokkaido University (No. 15A1004). The EXAFS experiments were carried out at beamline station BL-NW14A with the approval of PF-PAC (Prop. Nos. 2013G166, 2015G541, 2015G542).

Supporting Information is available on http://dx.doi.org/10.1246/cl.******.

References

1 *Heterogeneous Photocatalysis: From Fundamentals to Applications in Energy Conversion and Depollution*, ed. by J. Strunk, John Wiley and Sons, New York, **2021**.
2 T. Yokoyama, Y. Uemura, in XAFS Techniques for Catalysts, Nanomaterials, and Surfaces, ed. By Y. Iwasawa, K. Asakura, M. Tada, Springer, New York, **2017**, pp. 127–132.
3 R. Abe, Recent progress on photocatalytic and photoelectrochemical water splitting under visible light irradiation, J. Photochem. Photobiol. C **2010**, *11,* 179.
4 Y. Uemura, H. Uehara, Y. Niwa, S. Nozawa, T. Sato, S. Adachi, B. Ohtani, S. Takakusagi, K. Asakura, *Chem.Lett.* **2014**, *43*, 977.
5 Y. Uemura, D. Kido, Y. Wakisaka, H. Uehara, T. Ohba, Y. Niwa, S. Nozawa, T. Sato, K. Ichiyanagi, R. Fukaya, S.-i. Adachi,T. Katayama, T. Togashi, S. Owada, K. Ogawa, M. Yabashi,K. Hatada, S. Takakusagi, T. Yokoyama, B. Ohtani, K. Asakura, *Angew. Chem. Int. Ed.* **2016**, *55*, 1364.
6 A. Koide, Y. Uemura, D. Kido, Y. Wakisaka, S. Takakusagi, B. Ohtani, Y. Niwa, S. Nozawa, K. Ichiyanagi, R. Fukaya, S.-i. Adachi, T. Katayama, T. Togashi, S. Owada, M. Yabashi, Y. Yamamoto, M. Katayama, K. Hatada, T. Yokoyama, K. Asakura, *Phys. Chem. Chem. Phys*. **2020**, *20*, 2615.
7 Y. Uemura, T. Yokoyama, T. Katayama, S. Nozawa, K. Asakura, *Appl. Sci.* **2020**, *10*, 7818.
8 I. Bedja, S. Hotchandani, P. V. Kamat, *J. Phys. Chem.* **1993**, *97*, 11064.
9 *XAFS Techniques for Catalysts, Nanomaterials, and Surfaces*, ed. by Y. Iwasawa, K. Asakura, M. Tada, Springer Nature, New York, **2016**.
10 D. Kido, Y. Uemura, Y. Wakisaka, H. Ariga-Miwa, S. Takakusagi, K. Asakura, *e-J. Surf. Sci. Nanotech.* **2020**, *18*, 249.
11 D. Kido, M. M. Rahman, T. Takeguchi, K. Asakura, *Chem. Lett.* **2022**, *51*, 538.
12 K. Asakura, *in X-Ray Absorption Fine Structure for Catalysts and Surfaces, 1st ed. vol. 2,* ed. by Y. Iwasawa, World Scientific, Singapore, **1996**, pp.33–58.
13 M. Newville, *J. Phys.: Conf. Ser*. **2013**, *430*, 012007.
14 E. A. Stern, *Phys. Rev. B* **1993**, *48*, 9825.
15 D. Kido, K. Asakura, Acc. Mater. & Surf.Res. 2020, 5, 148.
16 I. Brown, *Chem. Soc. Rev.* **1978**, *7*, 359.
17 C. J. Howard, V. Luca, K. S. Knight, *J. Phys., Cond, Mat.* **2001**, *14*, 377.
18 Y. Obara, H. Ito, T. Ito, N. Kurahashi, S. Thurmer, H. Tanaka, T. Katayama, T. Togashi, S. Owada, Y. Yamamoto, S. Karashima, J. Nishitani, M. Yabashi, T. Suzuki, K. Misawa, *Struct. Dyn.* **2017**, *4*, 044033.
19 K. Sato, K.-i. Yamanaka, S. Nozawa, H. Fukuzawa, T. Katayama, T. Morikawa, T. Nonaka, K. Dohmae, K. Ueda, M. Yabashi, R. Asahi, *Inorg. Chem.* **2020**, *59*, 10439.
20 T. J. Penfold, J. Szlachetko, F. G. Santomauro, A. Britz, W. Gawelda, G. Doumy, A. M. March, S. H. Southworth, J. Rittmann, R. Abela, M. Chergui, C. J. Milne, *Nat. Commun.* **2018**, *9*, 478.
21 K. Kato, Y. Uemura, K. Asakura, A. Yamakata, *J. Phys. Chem. C.* **2022**, *126*, 9257.
22 Y. Uemura, A. S. M. Ismail, S. H. Park, S. Kwon, M. Kim, Y. Niwa, H. Wadati, H. Elnaggar, F. Frati, T. Haarman, N. H¨oppel, N. Huse, Y. Hirata, Y. Zhang, K. Yamagami, S. Yamamoto, I. Matsuda, T. Katayama, T. Togashi, S. Owada, M. Yabashi, U. Halisdemir, G. Koster, T. Yokoyama, B. M. Weckhuysen, F. M. F. de Groot, *J. Phys. Chem. C* **2021**, *125*, 7329.
23 S. Biswas, S. Wallentine, S. Bandaranayake, L. R. Baker, *J. Chem. Phys.* **2019**, *151*, 104701.

NOTE *The diagram is acceptable in a colored form. Publication of the colored G.A. is free of charge.*
For publication, electronic data of the colored G.A. should be submitted. Preferred data format is EPS, PS, CDX, PPT, and TIFF.
If the data of your G.A. is "bit-mapped image" data (not "vector data"), note that its print-resolution should be 300 dpi.
You are requested to put a brief abstract (50-60words, one paragraph style) with the graphical abstract you provided, so that readers can easily understand what the graphic shows.

Graphical Abstract

Textual Information

A brief abstract (required)	The local structure of WO_3 photocatalyst in the photoexcited metastable state created 150 ps after laser irradiation have been determined by the pump-probe L_3-edge EXAFS and the constrained thorough search analysis. A highly distorted octahedral local structure was found whose one of the shortest W-O bonds being further shortened to 1.66 Å while the other five bonds were elongated even though theoretical calculations predicted the reverse change. We discuss this contradiction and propose a possible structure for the metastable state.
Title(required)	Metastable structure of photoexcited WO_3 determined by the pump-probe extended X-ray absorption fine structure spectroscopy and constrained thorough search analysis
Authors' Names(required)	Daiki Kido, Yohei Uemura, Yuki Wakisaka, Akihiro Koide, Hiromitsu Uehara, Yasuhiro Niwa, Shunsuke Nozawa, Kohei Ichiyanagi, Ryo Fukaya, Shin-ichi Adachi, Tokushi Sato, Harry Jenkins, Toshihiko Yokoyama, Satoru Takakusagi, Jun-ya Hasegawa, and Kiyotaka Asakura

Graphical Information